Effects of Presynaptic Mutations on a Postsynaptic Cacna1s Calcium Channel Colocalized with mGluR6 at Mouse Photoreceptor Ribbon Synapses

Dana Specht,[1,2] *Shu-Biao Wu,*[3] *Paul Turner,*[3] *Peter Dearden,*[3] *Frank Koentgen,*[4] *Uwe Wolfrum,*[5] *Marion Maw,*[3] *Johann Helmut Brandstätter,*[1] *and Susanne tom Dieck*[1,2]

Purpose. Photoreceptor ribbon synapses translate light-dependent changes of membrane potential into graded transmitter release via L-type voltage-dependent calcium channel (VDCC) activity. Functional abnormalities (e.g., a reduced electroretinogram b-wave), arising from mutations of presynaptic proteins, such as Bassoon and the VDCCα1 subunit Cacna1f, have been shown to altered transmitter release. L-type VDCCα1 subtype expression in wild-type and mutant mice was examined, to investigate the underlying pathologic mechanism.

Methods. Two antisera against Cacna1f, and a *Cacna1f* mouse mutant (*Cacna1f*ΔEx14-17) were generated. Immunocytochemistry for L-type VDCCα1 subunits and additional synaptic marker proteins was performed in wild-type, *Bassoon*ΔEx4-5 and *Cacna1f*ΔEx14-17 mice.

Results. Active zone staining at photoreceptor ribbon synapses with a panα1 antibody colocalized with staining for Cacna1f in wild-type mouse retina. Similarly, in the *Bassoon*ΔEx4-5 mouse, residual mislocalized staining for panα1 and Cacna1f showed colocalization. Unlike the presynaptic location of Cacna1f and panα1 antibody staining, the skeletal muscle VDCCα1 subunit Cacna1s was present postsynaptically at ON-bipolar cell dendrites, where it colocalized with metabotropic glutamate receptor 6 (mGluR6). Surprisingly, Cacna1s labeling was severely downregulated in the *Bassoon*ΔEx4-5 and *Cacna1f*ΔEx14-17 mutants. Subsequent analyses revealed severely reduced ON-bipolar cell dendritic expression of the sarcoplasmic reticulum Ca^{2+} ATPase Serca2 in both mouse mutants and of mGluR6 in the *Cacna1f*ΔEx14-17 mutant.

Conclusions. Presynaptic mutations leading to reduced photoreceptor-to-bipolar cell signaling are associated with disturbances in protein expression within postsynaptic dendrites. Moreover, detection of Cacna1s and Serca2 in ON-bipolar cell dendrites in wild-type animals suggests a putative role in regulation of postsynaptic Ca^{2+} flux. (*Invest Ophthalmol Vis Sci.* 2009;50:505–515) DOI:10.1167/iovs.08-2758

Photoreceptor ribbon synapses continuously translate light-dependent changes in membrane potential into graded release of transmitter. Several features of ribbon synapses reflect the functional requirement for high rates of tonic transmitter release and for transmission of signals over several orders of magnitude.[1,2] For example, the calcium-triggered fusion of neurotransmitter-filled vesicles at ribbon synapses is mediated by slowly inactivating L-type voltage-dependent calcium channels (VDCCs), rather than by the N- or P/Q-type channels present in conventional synapses.[3–7]

The central, pore-forming component of a VDCC is provided by the α1 subunit. Of the 10 known VDCCα1 subunits, four form L-type channels: Cacna1s ($Ca_v1.1$), Cacna1c ($Ca_v1.2$), Cacna1d ($Ca_v1.3$), and Cacna1f ($Ca_v1.4$).[7] Loss-of-function mutations in the human *CACNA1F* gene cause the incomplete form of X-linked congenital stationary night blindness (CSNB2).[8,9] The condition is characterized by an electroretinogram (ERG) with a largely intact a-wave and a highly reduced b-wave, which indicates defective transmission of light signals from photoreceptors to second-order neurons. In the rodent, Cacna1f immunoreactivity has been detected at photoreceptor presynaptic sites,[10,11] and loss-of-function mutations in the murine *Cacna1f* gene result in ERG b-wave reduction and in cellular and morphologic changes at the photoreceptor synapse.[12,13]

Aside from CACNA1F/Cacna1f, mutations in various other genes for ribbon synaptic proteins lead to retinal dysfunction with a reduced ERG b-wave in mice, zebrafish, and/or humans.[14–22] In the Bassoon mouse mutant *Bsn*ΔEx4-5, the photoreceptor ribbons are not anchored to the presynaptic active zone and float freely in the cytoplasm.[15] In addition, clustering of active zone proteins in the arciform density/plasma membrane compartment is decreased and proteins are mislocalized, which results in the loss of the horseshoe-shaped outline of the active zone.[23] One of the mislocalized proteins in the *Bsn*ΔEx4-5 mutant is a VDCCα1 subunit stained with the panα1 antiserum (CP15), most likely the Cacna1f subunit.[23] Thus, the *Bsn*ΔEx4-5 phenotype could result at least in part from mislocalization of Cacna1f.

In this study, we asked whether the protein selectively stained by the panα1(CP15) antiserum is truly Cacna1f. Although the $Ca_v1.4$ channel with its unique biophysical properties is undoubtedly the most important VDCC for retinal photoreceptor to bipolar cell transmission,[7–10,24,25] the assumption that panα1 staining corresponds to Cacna1f protein requires direct examination for several reasons:

1. The panα1(CP15) antibody is directed against a conserved epitope within the binding domain for the auxiliary $\alpha2\delta$ subunit, but epitope masking impedes interpre-

From the [1]Department of Biology, Animal Physiology, University of Erlangen-Nuremberg, Erlangen, Germany; the [2]Department of Neuroanatomy, Max Planck Institute for Brain Research, Frankfurt/Main, Germany; the [3]Department of Biochemistry, University of Otago, Dunedin, New Zealand; [4]Ozgene Pty. LtD, Bentley, Western Australia, Australia; and the [5]Department of Cell and Matrix Biology, Institute of Zoology, Johannes Gutenberg University of Mainz, Mainz, Germany

Supported by Grant BR 1643/4-1 from Deutsche Forschungsgemeinschaft (JHB); FAUN-Stiftung, Nürnberg (UW); and by grants from the Lottery Grants Board of New Zealand, Retina Australia, the Maurice and Phyllis Paykel Trust, the Health Research Council of New Zealand, and the University of Otago (MM).

Submitted for publication August 21, 2008; revised September 23, 2008; accepted December 3, 2008.

Disclosure: **D. Specht**, None; **S.-B. Wu**, None; **P. Turner**, None; **P. Dearden**, None; **F. Koentgen**, Ozgene Pty., Ltd. (E, F); **U. Wolfrum**, None; **M. Maw**, None; **J.H. Brandstätter**, None; **S. tom Dieck**, None

The publication costs of this article were defrayed in part by page charge payment. This article must therefore be marked "*advertisement*" in accordance with 18 U.S.C. §1734 solely to indicate this fact.

Corresponding author: Susanne tom Dieck, MPI for Brain Research, Department of Neuroanatomy, Deutschordenstrasse 46, D-60528, Frankfurt/Main, Germany; tomdieck@mpih-frankfurt.mpg.de.

tation of Western blot and immunocytochemistry data. Evidence that multiple VDCCs are expressed in various cell types in rodent retina[5,11,25–30] stands in contrast to selective staining of photoreceptor and bipolar cell presynaptic active zones with the panα1(CP15) antibody.[23] Hence, the ribbon active zone staining could reflect a VDCCα1 subunit other than Cacna1f.

2. Photoreceptor synaptic transmission is not completely blocked by *CACNA1F/ Cacna1f* mutations. It has thus been suggested that other L-type VDCCs may be responsible for residual transmission.[11,13] Cacna1d, which is most similar to Cacna1f, was detected immunocytochemically at cone synapses in mice, and other studies suggest an even broader distribution.[11,28,31]
3. Retinal staining patterns and molecular weight estimates with different CACNA1F/Cacna1f antibodies described to date vary and do not necessarily include photoreceptor presynaptic active zone staining.[10,11,25,27,32]

To determine which VDCCα1 subunit is mislocalized in Bassoon mutant photoreceptor synapses, we raised new antisera to Cacna1f and generated a mouse with a deletion mutation in the *Cacna1f* gene. These tools were used to compare staining patterns of L-type VDCC antibodies in retinal sections from wild-type and Bassoon- and Cacna1f-deficient mice.

METHODS

All animal experiments were performed in compliance with the ARVO Statement for the Use of Animals in Ophthalmic and Vision Research and the guidelines issued by the University of Erlangen-Nuremberg.

Generation of *Cacna1f*ΔEx14-17 Mice

The targeting vector was designed to produce both a mouse model for an I745T *CACNA1F* mutation identified in a New Zealand family[33] and a *Cacna1f*-deficient line. The targeting vector was constructed in a vector (pBluescriptSK; Stratagene, La Jolla, CA), with PCR fragments spanning the Cacna1f genomic region from exon 8 to intron 21 amplified from C57BL/6 mouse spleen DNA. A point mutation coding for the Ile to Thr exchange and a neomycin resistance cassette with PGK promoter flanked by FRT sites were introduced into, respectively, exon 17 and intron 17 and flanked by loxP sites in introns 13 and 17. The targeting vector was introduced into a C57BL/6 ES cell line derived from mouse strain C57BL/6-Thy1.1[34] and screened for homologous recombination. The mouse line generated from targeted embryonic stem (ES) cells was subsequently crossed to Cre recombinase-expressing mice to excise the region flanked by loxP sites resulting in the removal of exons 14 to 17 (see also Fig 2A).

Antibodies

For generation of sheep (sh) anti-Cacna1f(Pep1) and rabbit (rb) anti-Cacna1f(Pep3) antibodies, animals were immunized with Pep1 (SSEGNPPKENKVLVPGGEN, the murine version of a human CACNA1F peptide located in the cytoplasmic loop between domains II and III used in Morgans et al.,[27]) and Pep3 (AEEGRAGHRPQLSELTN, a Cacna1f-specific peptide located in the cytoplasmic loop between domains I and II) coupled to diphtheria toxoid and KLH, respectively. Antibodies were affinity purified using the immunizing peptides and were applied in immunocytochemistry (ICC), Western blot (WB), and pre-embedding immunoelectron microscopy (pre-EM) in the following dilutions: sh anti-Cacna1f(Pep1) (1:1000 ICC), rb anti-Cacna1f(Pep3) (1:5000 ICC; 1:1000–1:5000 WB); rb anti-panα1 (1:500 ICC; 1:200 WB; Chemicon, Temecula, CA), ms anti-Cacna1s (mab1A, 1:5000 ICC, pre-EM; 1:300 WB; Chemicon), rb anti-Cacna1d (1:1000 ICC; Chemicon and Alomone, Jerusalem, Israel), rb anti-Cacna1c (1:100 ICC; 1:200 WB; Chemicon and Alomone), rb anti-PKCα (1:1000 ICC; Sigma-Aldrich, St. Louis, MO), rb anti-mGluR6 (1:100 ICC; Neuromics, Edina, MN), rb anti-Veli3 (1:1000 ICC; Zymed, San Francisco, CA), ms anti-CtBP2/RIBEYE (1:10,000 ICC; BD Biosciences, Heidelberg, Germany), gp anti-Piccolo[35] (1:800 ICC, kindly provided by Eckart Gundelfinger, Leibniz Institute for Neurobiology, Magdeburg, Germany), ms anti-Bassoon (mab7f, 1:2500 ICC; Stressgen, Victoria, BC, Canada), rb anti-Calbindin (1:1000 ICC; Swant, Bellinzona, Switzerland), rb anti-Serca2 (1:1000 ICC; Sigma-Aldrich), rb anti-Vlgr1/Gpr98[36] (1:1000 ICC), and ms anti-β-dystroglycan (1:500 ICC; Novocastra, Newcastle-upon-Tyne, UK).

Secondary antibodies were raised in goat or donkey and coupled to Alexa488 or Alexa594 (1:500; Invitrogen-Molecular Probes, Eugene, OR) for ICC, to biotin (1:500; Vector, Burlingame, CA) for pre-EM and to horseradish peroxidase (gt anti-rb HRP, 1:40,000; New England Biolabs; gt anti-ms HRP, 1:30,000; Sigma-Aldrich) for WB.

Retinal Tissue Preparation and Light and Electron Microscopic Immunocytochemistry

Mice were kept in a 12:12 light–dark cycle (light onset, 6 am) and killed for experiments at the ages indicated in the morning by decapitation after deep anesthesia with isoflurane. At least three animals of each genotype were analyzed at each age. Generation of the *Bsn*ΔEx4-5 mutant mice by gene targeting has been described.[37] Homozygous *Bsn*ΔEx4-5 mice and wild-type littermate controls (mixed background: C57Bl/6 and 129/Sv x 129/SvJ from R1 ES-cells) were obtained as offspring from intercrosses of heterozygous *Bsn*ΔEx4-5 mice. Hemizygous male or homozygous female *Cacna1f*ΔEx14-17 mice (termed *Cacna1f*ΔEx14-17 together; background: C57Bl/6) were obtained from heterozygote x hemizygote intercrosses and from crosses of C57Bl/6 males to heterozygous *Cacna1f*ΔEx14-17 females. Wild-type controls were obtained from the same litters. Although mutants were always analyzed in parallel with the wild-type littermate control, in experiments without mutants, wild-type animals were from the C57Bl/6 strain.

For light microscopy after anesthesia and decapitation, eyes were dissected and retinas were immersion fixed in the eye cup in 4% (wt/vol) paraformaldehyde (PFA) in phosphate buffer (PB; 0.1 M; pH 7.4) for 15 or 30 minutes or ice-cold methanol for 30 minutes (Serca2 and Cacna1d labeling) after removal of cornea, lens, and vitreous. After washes in phosphate-buffered saline (PBS; 0.01 M; pH 7.4), the pigment epithelium was removed and the retinas were cryoprotected in increasing concentrations of sucrose in PBS (10%, 20%, and 30%) at 4°C before being frozen in freezing medium (Reichert-Jung, Bensheim, Germany) as sandwiches of wild-type and mutant material. Vertical sections of 14-μm thickness were cut on a cryostat (Leica Microsystems, Nussloch, Germany), collected on slides, and stored at −20°C. Preparation of retinal tissue for electron microscopy and antibody incubation for light and electron microscopic immunocytochemistry was performed according to established procedures.[35,38] For peptide blocking experiments, the antibodies were preincubated for 1 hour on ice, with or without the respective peptides before overnight incubation at room temperature.

For light microscopic analysis, labeled sections were examined with a confocal laser scanning microscope (LSM5 Pascal; Carl Zeiss Meditec, Oberkochen, Germany). Images were adjusted for contrast and brightness (Photoshop CS; Adobe Systems, San Jose, CA), and the figures were arranged (Draw X3; Corel, Ottawa, ON, Canada). For electron microscopic analysis, ultrathin sections were examined and photographed with an electron microscope (EM10; Carl Zeiss Meditec) and a digital camera (BioScan; Gatan, Munich, Germany) in combination with software (Digital Micrograph 3.1; Gatan).

Western Blot

For Western blot analysis of retina homogenate, the retinas were homogenized in extraction buffer (50 mM Tris-HCl [pH 7.5], 150 mM NaCl, 1% TritonX-100, 0.5% Na-deoxycholate, and protease inhibitors), total protein was precipitated with trichloroacetic acid, dissolved in sample buffer, separated on 3% to 8% tris-acetate gels (25 μg/lane;

Novex; Invitrogen, Carlsbad, CA), and transferred to PVDF membranes by tank blotting.[37] Crude membrane fractions were prepared by centrifugation (20 minutes, 12.000*g*) of the postnuclear supernatant (10 minutes, 1000*g*) of a tissue homogenate in 0.32 M sucrose and 5 mM HEPES (pH 7.4). The crude membrane pellet was dissolved in sample buffer and separated. For immunodetection, membranes were blocked and primary antibodies were applied overnight at 4°C. The HRP-coupled secondary antibodies were visualized by chemiluminescence detection (GE Healthcare, Freiburg, Germany).

RT-PCR and Northern Blot

Expression of *Cacna1s* transcripts was shown by RT-PCR performed on total retinal and skeletal muscle RNA (RNAeasy Kit; Qiagen, Hilden, Germany) with two *Cacna1s*-specific primer pairs (554-bp fragment: forward 5′-ACA TGC CTG TTA CCA GAG AAG GAC-3′; reverse, 5′-TCT GTA TAG GCC CTC ACA TCT GG-3′; an initial step of 30 seconds at 98°C followed by 30 cycles of 10 seconds at 98°C, 30 seconds at 58°C, 60 seconds at 72°C; 508-bp fragment: forward 5′-CTA CTT TGT CAC CCT CAT TCT GCT-3′; reverse 5′-TCA TGA GCA TTT GCA TGG TGA AGA-3′; an initial step of 30 seconds at 98°C followed by 30 cycles of 10 seconds at 98°C, 30 seconds at 64°C, and 60 seconds at 72°C).

The 508-bp fragment was cloned into a vector (pGemTeasy; Promega, Madison, WI) to produce a DIG-labeled RNA probe (DIG Northern Starter Kit; Roche, Mannheim, Germany) for hybridization of Northern blot analysis of total RNA from the retina, skeletal muscle, and liver (hybridization temperature 66°C, DIG Wash and Block buffer set; Roche).

Results

Photoreceptor ribbon synapses are located in the outer plexiform layer (OPL) of the retina. To compare staining of the panα1 serum with staining for the individual L-type VDCCα1 subunits in immunocytochemistry of retinal sections and Western blot analysis of whole tissue, we used commercially available antibodies for Cacna1c(CNC1), Cacna1d(AB5158), and Cacna1s(mab1A) and produced antisera against two peptides (Pep1, Pep3) from different regions of mouse Cacna1f (Fig. 1A).

As shown previously,[23] the panα1 antiserum strongly labeled discrete puncta in the OPL of wild-type mice (Fig. 1B). The affinity-purified Cacna1f(Pep1) and Cacna1f(Pep3) antisera exhibited comparable staining patterns with discrete spots in the OPL (Figs. 1C, 1D). A similar distribution in the OPL was also seen for the monoclonal antibody mab1A directed against Cacna1s,[39] together with staining in the perinuclear regions in the inner nuclear layer (INL) and the ganglion cell layer (GCL) (Fig. 1E). For all four antibodies, staining was blocked by preincubation with synthetic peptides of their respective epitopes (Figs. 1H–M).

Unlike Cacna1f and Cacna1s, staining patterns for Cacna1c and Cacna1d differed from, and did not overlap with, panα1 staining (Figs. 1F, 1G). The Cacna1c antiserum intensely labeled the rod bipolar cells (Figs. 1F, 1L), which is in agreement with an earlier study.[28]

A Cacna1d antiserum that showed immunoreactivity in hair cell ribbon synapses of the cochlea[6] gave diffuse but specific labeling in both synaptic layers of the retina (Fig. 1G, 1M) in agreement with results showing *Cacna1d* message broadly distributed in retinal cell types.[29,31] As selective staining of cone active zones was recently shown with a different Cacna1d antiserum,[11] several Cacna1d forms are presumably present in the mouse retina. Our data, however, suggest that they are most likely not labeled by the panα1 antiserum.

In contrast to the immunocytochemistry findings, no common bands were detectable between the panα1 and Cacna1f(Pep3) antibodies in Western blot analysis of retinal extracts. Instead, the high-molecular-weight band for panα1 corresponded to that for Cacna1c (Fig. 1N).

Cacna1s, Cacna1f, and panα1 Staining in Cacna1f and Bassoon Mouse Mutants

We next compared the labeling patterns of the panα1, Cacna1f, and Cacna1s antibodies in the *Bsn*ΔEx4-5 mouse in which panα1 is mislocalized and separated from ribbon proteins[23] and in a newly generated mouse mutant in which *Cacna1f* exons 14 to 17 have been deleted, the *Cacna1f*ΔEx14-17 mouse (Fig. 2A). This modification removes the sequence encoding transmembrane segments 2 to 6 of domain II and part of the cytoplasmic loop between domains II and III and is predicted to introduce a frameshift followed by a premature stop codon (Fig. 2B). In line with the absence of a common band for panα1 and Cacna1f antisera in Western blot analysis of wild-type retina (Fig. 1N), a wild-type Cacna1f band did not disappear in the *Cacna1f*ΔEx14-17 mutant with either antibody (Fig. 2C). Thus, a full-length wild-type Cacna1f band is presumably not detectable under our Western blot conditions. However, a low-molecular-weight band absent in wild-type extracts appeared on Cacna1f(Pep3)- but not panα1-probed Western blot analysis (Fig. 2C) and could correspond to a N-terminal hypomorphic protein: such a protein would be predicted to contain the Pep3 sequence but to lack the C-terminal cytoplasmic epitope recognized by panα1 (Fig. 2B).

Unexpectedly, as with wild-type retina (Figs. 1B–E, 2D–F), the Cacna1f and the Cacna1s staining both behaved similarly to the panα1 staining in the two mouse models (Figs. 2G–S). The residual, mislocalized panα1, Cacna1f(Pep3) and Cacna1s staining in the *Bsn*ΔEx4-5 mutant was progressively lost with age (Figs. 2D–O). When compared with the *Bsn*ΔEx4-5 mutant (Figs. 2J–L), labeling in the 10-week-old *Cacna1f*ΔEx14-17 mutant retina was more severely reduced (Figs. 2P–S). Cacna1s labeling was at background levels (Fig. 2S). Of note, Cacna1f(Pep1) (Fig. 2P), and panα1 (Fig. 2Q) labeling was also at background levels, whereas rare spots of residual Cacna1f(Pep3) immunoreactivity were found in the OPL of *Cacna1f*ΔEx14-17 mutants (Fig. 2R). This residual Cacna1f(Pep3) staining was blocked by preincubation with the immunizing peptide (not shown). These latter findings were again consistent with expression in the *Cacna1f*ΔEx14-17 mutant of a putative N-terminal hypomorphic protein, which would be predicted to lack the Pep1 and panα1 epitopes (Fig. 2B).

Postsynaptic Cacna1s at the Photoreceptor Ribbon Synapse

As with wild-type retina, the staining patterns for the VDCCα1 antibodies in the two mouse mutants were compatible with panα1 labeling of Cacna1f and/or Cacna1s protein (Fig. 2). Next, we used high-resolution confocal microscopy and double-labeling experiments to compare the subcellular localizations of the panα1, Cacna1f, and Cacna1s epitopes (Figs. 3, 4).

The rod spherule usually contains a single large synaptic ribbon, which bends, together with the active zone/arciform density, around deeply invaginating postsynaptic elements consisting of the dendrites and processes of bipolar and horizontal cells, respectively (Fig. 3A). This formation results in a horseshoe-shaped structure that is clearly visible at the light microscopic level.[2] Both panα1 and Cacna1f(Pep3) showed a horseshoe-shaped staining, which overlapped with staining for the presynaptic active zone/arciform density marker Bassoon (Figs. 3B, 3C) and which was slightly shifted to the inside of the horseshoe when compared to staining for the ribbon markers RIBEYE (Figs. 3D, 3E) and Piccolo (Figs. 3F, 3G). Hence these findings established a presynaptic arciform density/plasma membrane localization for both VDCCα1 epitopes.

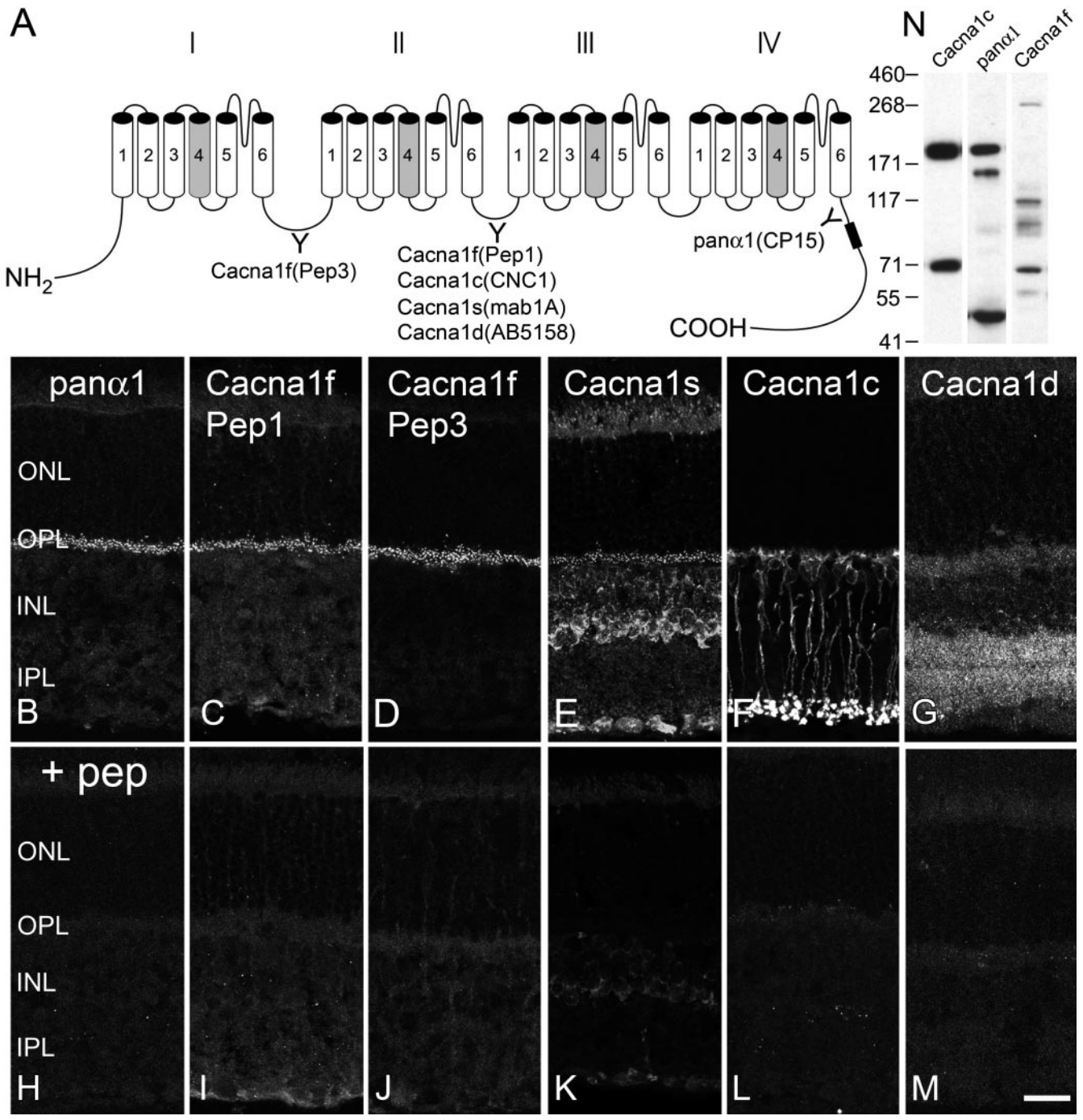

FIGURE 1. Voltage-dependent calcium channel (VDCC)α1 subunit staining patterns in wild-type mouse retina. (**A**) The VDCCα1 subunit topology, showing domains I–IV, each containing six transmembrane segments, with the approximate positions of antibody epitopes. (**B–M**) Confocal laser scanning micrographs of vertical cryostat sections through wild-type mouse retina stained with antibodies against L-type VDCCα1 subunits (**B–G**) and the respective peptide preincubation controls (**H–M**). (**N**) Western blot of total protein extract from wild-type retina (25 μg/lane) stained with Cacna1c, panα1, and Cacna1f(Pep3) antibodies; the position of molecular weight standards (kDa) is indicated. Scale bar, 20 μm.

In contrast to the presynaptic panα1 and Cacna1f staining (Fig. 3), high-resolution confocal microscopy for Cacna1s revealed postsynaptic labeling of the photoreceptor ribbon synapses (Fig. 4). Double-labeling demonstrated that the Cacna1s-stained puncta lie beneath the arc described by the ribbon (Piccolo, Fig. 4A) and active zone/plasma membrane (Cacna1f(Pep3), Fig. 4B), and within the area outlined by the rod terminal (Veli3; Fig. 4C). Further double-labeling experiments combining Cacna1s staining with labeling for postsynaptic horizontal cell processes (calbindin; Fig. 4D), bipolar cell dendrites (PKCα; Fig. 4E), and ON-bipolar cell dendritic tips (mGluR6, Fig. 4F), unambiguously demonstrated a postsynaptic localization for Cacna1s in the dendritic tips of rod and ON-cone bipolar cells. The postsynaptic localization of Cacna1s was confirmed by pre-embedding immunoelectron microscopy. The invaginating dendrites of ON-bipolar cells postsynaptic at rod and cone terminals, respectively, were strongly labeled for Cacna1s, whereas the invaginating processes of horizontal cells were free of labeling (Figs. 4G, 4H). Hence, in

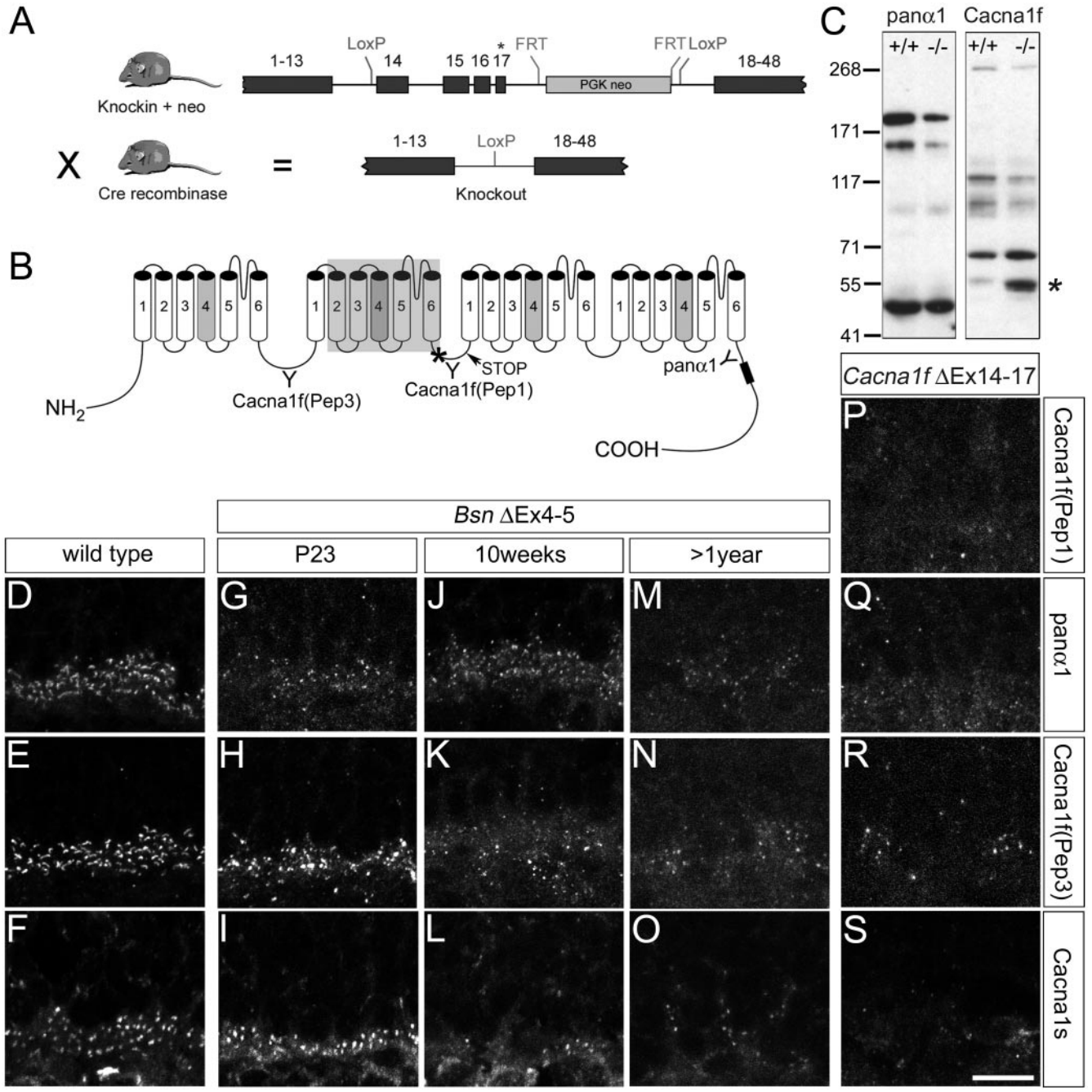

FIGURE 2. Reduction of panα1, Cacna1f, and Cacna1s immunoreactivity in *Bsn*ΔEx4-5 and *Cacna1f*ΔEx14-17 mouse mutants. (**A**) The breeding strategy to generate the *Cacna1f*ΔEx14-17 mouse mutant. The parent line contained a point mutation in exon 17 coding for an Ile to Thr amino acid exchange (✶) and a neo cassette with FRT sites in intron 17 which were flanked by loxP sites in intron 13 and 17. A cross with Cre recombinase-expressing mice removed the sequences between the loxP sites, generating the *Cacna1f*ΔEx14-17 mouse line. (**B**) Location of the Pep1 and Pep3 sequences and the epitope recognized by panα1 in the Cacna1f polypeptide, relative to the modification encoded by the *Cacna1f*ΔEx14-17 allele. *Shaded box*: sequence encoded by the deleted exons; ✶, predicted frameshift; *arrow*, predicted stop codon. (**C**) Comparison of Western blot analysis from wild-type (+/+) and *Cacna1f*ΔEx14-17 (−/−) retina extract stained with Cacna1f(Pep3) and panα1. ✶, A lower molecular weight band detected in *Cacna1f*ΔEx14-17 retina with Cacna1f(Pep3) but not panα1. (**D–S**) Confocal laser scanning micrographs of the OPL region of vertical cryostat sections from 10-week-old wild-type retina (**D–F**), *Bsn*ΔEx4-5 retina at different ages (**G–O**), and 10-week-old *Cacna1f*ΔEx14-17 retina (**P–S**) stained with panα1, Cacna1f(Pep3), Cacna1f(Pep1), and Cacna1s. Scale bar, 10 μm.

retinal immunocytochemistry, the panα1 antiserum reflects Cacna1f rather than Cacna1s staining.

We sought evidence, in addition to peptide block (Fig. 1K), that the mab1A staining in the OPL reflects the presence of Cacna1s protein. Northern blot analysis faintly showed retinal transcripts of the same size as detected in skeletal muscle (Fig. 4I). Moreover, RT-PCR using retinal RNA with subsequent sequencing confirmed *Cacna1s* expression in the retina (not shown). Western blot analysis of membrane fractions showed extremely strong staining of skeletal muscle, and weak staining of heart, whereas expression near detection threshold was seen for retina and brain (Fig. 4J).

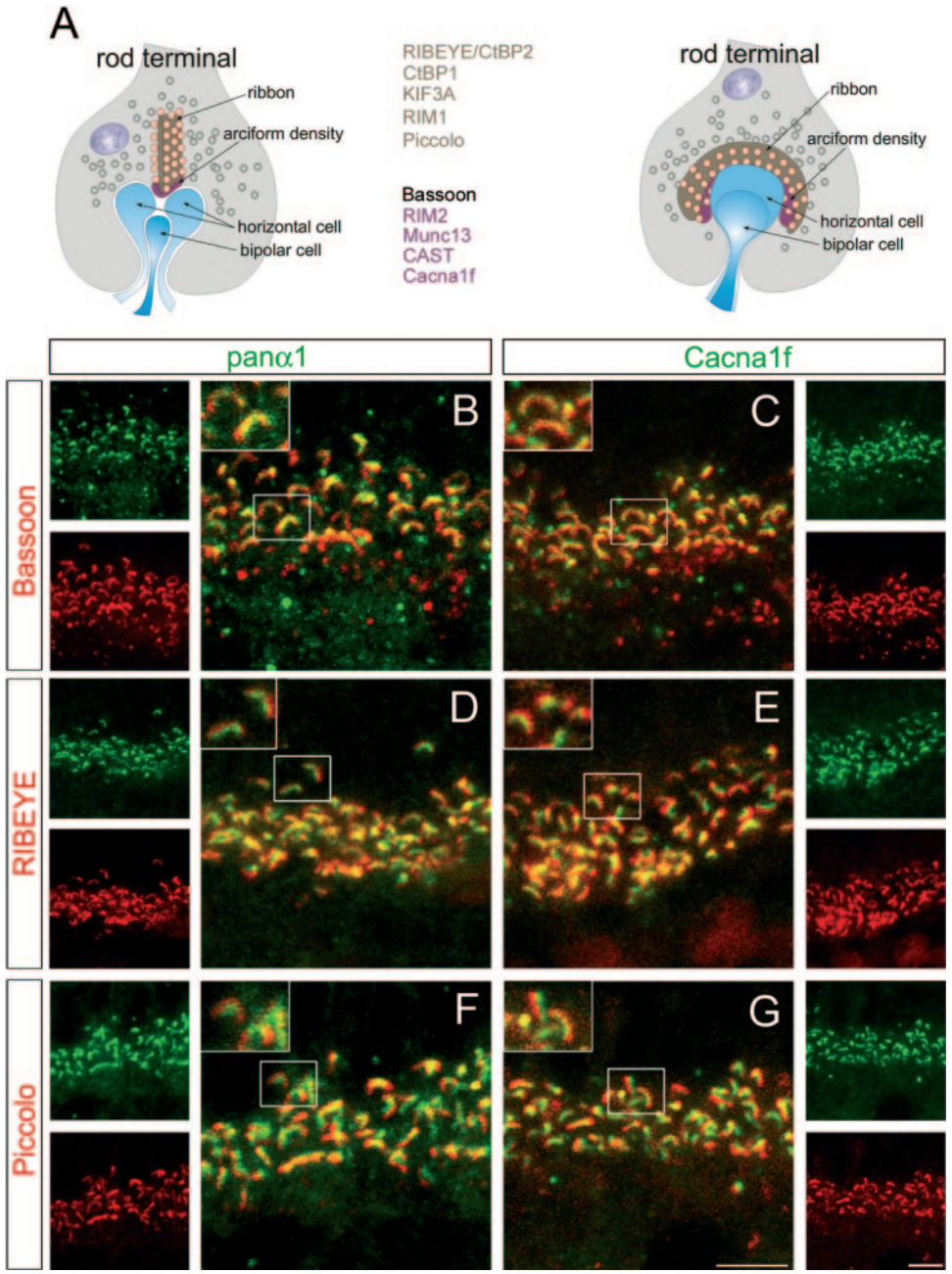

FIGURE 3. Cacna1f and panα1 antibodies stained the same presynaptic compartment. (**A**) A rod spherule with synaptic elements in two section planes and proteins localized to the horseshoe-shaped ribbon and arciform density compartments. (**B–G**) High-power confocal laser scanning micrographs of the OPL in vertical cryostat sections through wild-type retina labeled with panα1 (**B**, **D**, **F**) or Cacna1f(Pep3) (**C**, **E**, **G**), together with the arciform density marker Bassoon (**B**, **C**) and the ribbon markers RIBEYE (**D**, **E**), and Piccolo (**F**, **G**). Scale bar, 5 μm.

Postsynaptic Changes in Cacna1f and Bassoon Mouse Mutant Retinas

The postsynaptic localization of Cacna1s, together with the reduced Cacna1s staining in the Bassoon and Cacna1f mutant mice (Fig. 2), revealed that expression of a postsynaptic VDCCα1 subunit is affected by deficiency of these presynaptic proteins. To further investigate the extent of postsynaptic alterations, we searched for additional proteins localized at the invaginating dendrites of ON-bipolar cells (Fig. 5). In wild-type retina, we found a labeling pattern similar to Cacna1s (Fig. 5A) and mGluR6 (Fig. 5B) for a sarcoplasmic reticulum Ca^{2+} ATPase (Serca2)[40] (Fig. 5C), for very large G protein-coupled receptor 1/G protein-coupled receptor 98 (Vlgr1/Gpr98)[41] (Fig. 5D) and for the photoreceptor synapse extracellular matrix component dystroglycan[42,43] (Fig. 5E).

In the *Bsn*ΔEx4-5 retina of adult animals, labeling for Cacna1s and Serca2 was severely reduced (Figs. 5F, 5H), whereas mGluR6, Vlgr1/Gpr98, and dystroglycan were still localized within the synapses in the OPL, with additional immunoreactive puncta also present at ectopic sites in the ONL (Figs. 5G, 5I, 5J). In the adult *Cacna1f*ΔEx14-17 retina, the staining patterns for all five proteins were severely compromised (Figs. 5K–O). Labeling of Cacna1s, mGluR6, Serca2, and dystroglycan was highly reduced and diffuse with only occasional dotlike staining (Figs. 5K–M, 5O). Vlgr1/Gpr98 immunoreactivity was retained, but was located at larger unidentified structures rather than being concentrated in small spots that could have corresponded to bipolar cell dendritic tips (Fig. 5N).

DISCUSSION

Cacna1f at the Photoreceptor Active Zone

In the present study, antibodies against two Cacna1f-specific peptides, and against the conserved panα1(CP15) epitope but

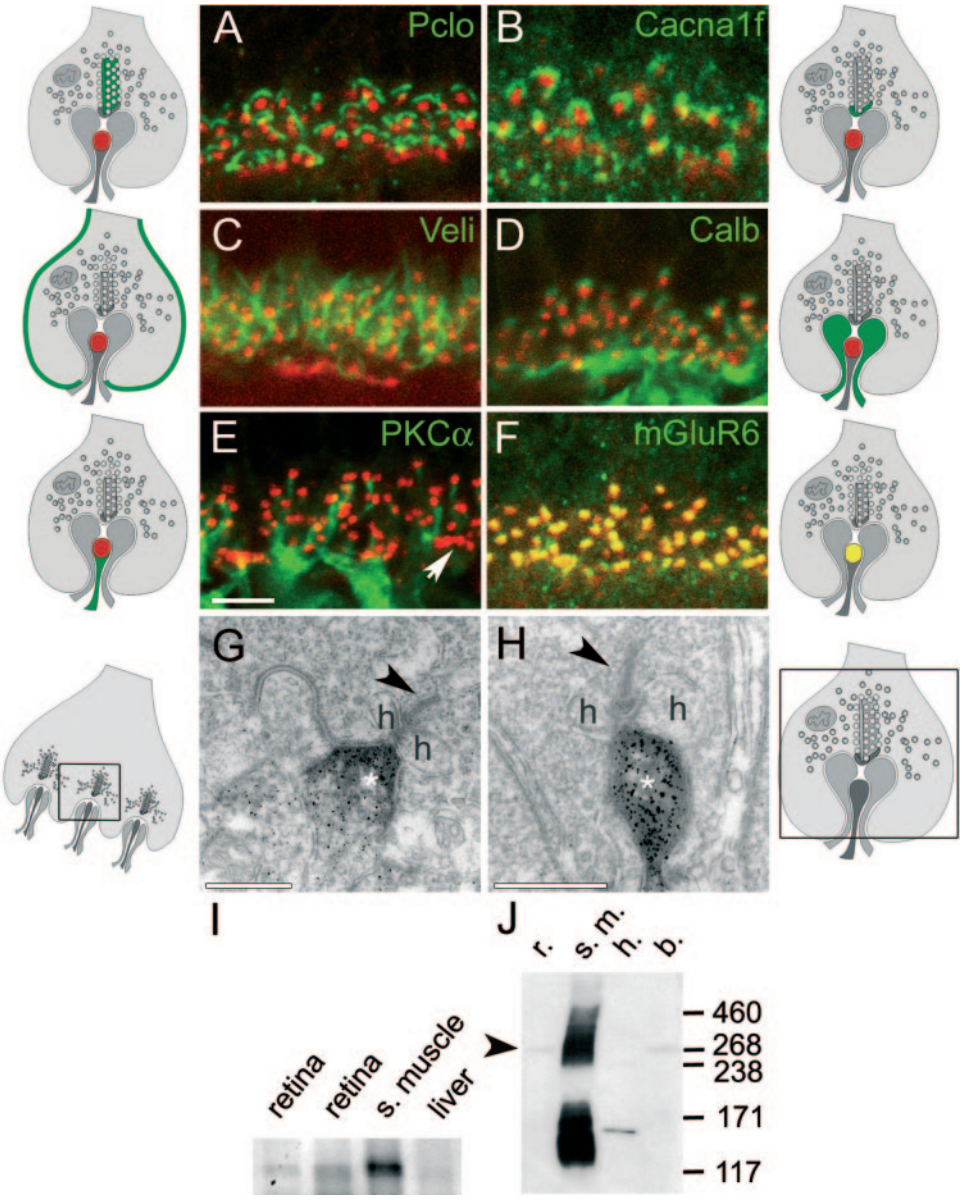

FIGURE 4. Cacna1s was localized postsynaptically at bipolar cell dendritic tips. (**A–F**) High-power confocal laser scanning micrographs of the OPL in vertical cryostat sections through mouse retina double labeled for Cacna1s (*red*) and markers of distinct synapse compartments (*green*) as indicated in the schematic drawings; (**A**) Piccolo, ribbon. (**B**) Cacna1f, presynaptic active zone/plasma membrane. (**C**) Veli3, rod terminal membrane. (**D**) calbindin, horizontal cells. (**E**) PKCα, rod bipolar cells. (**F**) mGluR6, ON-bipolar cell dendritic tip. (**G**, **H**) Electron micrographs of a cone pedicle (**G**) and a rod spherule (**H**) labeled for Cacna1s by the preembedding technique. ✶, Invaginating ON-bipolar cell dendritic tips; h, horizontal cells; *arrowhead*, photoreceptor synaptic ribbon. (**I**) Northern blot detection of *Cacna1s* transcripts in total RNA (retina, 2 μg; retina, 8 μg; skeletal muscle, 1 μg; liver, 2 μg). (**J**) Western blot of crude membrane fractions (25 μg/lane) from retina, skeletal muscle, heart and brain incubated with the Cacna1s antibody. Only faint bands (*arrowhead*) were present in retina and brain, at a molecular weight corresponding to the high molecular weight band in skeletal muscle; and in heart, at a molecular weight corresponding to the lower molecular weight band in skeletal muscle. The position of molecular weight standards (kDa) is indicated. Scale bars, (**A–F**) 5 μm; (**G**, **H**) 0.5 μm. PKC, protein kinase C; mGluR, metabotropic glutamate receptor.

none of the other L-type VDCCα1 subunits resulted in horseshoe-shaped photoreceptor active zone staining. Moreover, synaptic staining with all three antibodies was reduced in Bassoon- and Cacna1f-deficient mice. Collectively, these findings support a growing body of evidence that Cacna1f is expressed at the rodent photoreceptor ribbon synapse active zone.

Postsynaptic VDCC at the Photoreceptor Synapse

Unexpectedly, we found a postsynaptic VDCCα1 epitope at the photoreceptor synapse with the Cacna1s antibody mab1A. Cacna1s was present at ON-bipolar cell dendritic invaginations. Retention of correct mGluR6 and dystroglycan localization and of Vlgr1/Gpr98 labeling indicates that loss of Cacna1s and Serca2 staining is a relatively specific postsynaptic alteration in the *Bsn*ΔEx4-5 mutant. In skeletal muscle, Cacna1s/Ca_v1.1 acts primarily as a voltage sensor for ryanodine receptor 1 (RyR1) rather than as a VDCC. RyR1 mediates release of Ca^{2+} from intracellular stores, which is then pumped back to the sarcoplasmic reticulum by the Ca^{2+} ATPase Serca.[40] However, we found no specific enrichment of RyRs in ON-bipolar cell dendritic tips, as also observed in other studies.[44,45] Hence, the Ca_v1.1 channel is unlikely to act as a voltage sensor for ryanodine receptors in this context. Cacna1s/Ca_v1.1 plays an additional adaptive role in muscle fibers, because VDCC activity is greatly enhanced via phosphorylation after repetitive stimulation.[46] Accordingly, Ca_v1.1 could conceivably act in the ON-bipolar cell dendritic compartment as a VDCC and, together with Serca2, may regulate Ca^{2+} flux.

Cacna1s colocalized with the G protein-coupled receptors mGluR6 and Vlgr1/Gpr98, which are mutated in forms of congenital stationary night blindness and Usher syndrome, respectively.[19,21,41] Given that VDCCs can be regulated by G protein-coupled receptors,[47–49] it is tempting to speculate that a functional link exists. In the dark, glutamate released by photoreceptors binds to the metabotropic glutamate receptor mGluR6 at ON-bipolar cell dendrites.[50,51] Subsequently, mGluR6 activates a G protein pathway, which leads to hyperpolarization of the ON-bipolar cell.[52–56] Modulation of this signaling pathway enables adaptation to the level of illumination.[57,58] Of interest here is that Ca^{2+} triggers rundown of the glutamate response, via repolarization of the synaptic poten-

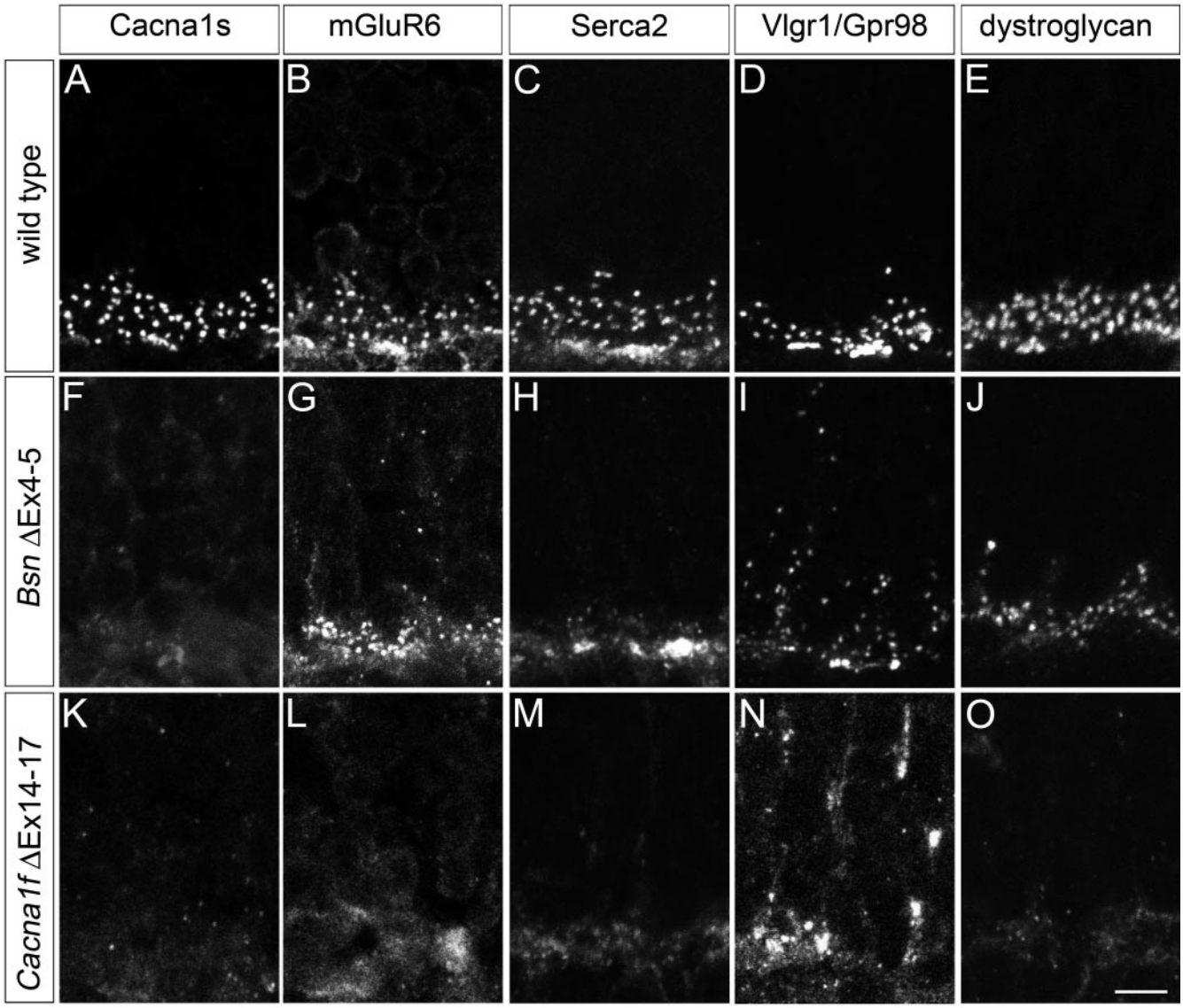

FIGURE 5. Post- and transsynaptic changes in *Bsn*ΔEx4-5 and *Cacna1f*ΔEx14-17 mutant retinas. Confocal laser scanning micrographs of vertical cryostat sections through adult wild-type (**A**–**E**), *Bsn*ΔEx4-5 (**F**–**J**), and *Cacna1f*ΔEx14-17 (**K**–**O**) retinas stained for proteins associated with postsynaptic invaginations: (**A**, **F**, **K**) Cacna1s, (**B**, **G**, **L**) mGluR6, (**C**, **H**, **M**) Serca2, (**D**, **I**, **N**) Vlgr1/Gpr98, and (**E**, **J**, **O**) the ECM linker dystroglycan. Scale bar, 5 μm. Serca, sarcoplasmic reticulum Ca^{2+} ATPase; Vlgr, very large G protein-coupled receptor; Gpr, G protein-coupled receptor; ECM, extracellular matrix.

tial. The exact mechanism is unclear, but may involve calcineurin.[57–61] Hence, $Ca_v1.1$ and Serca2 could contribute to ON-bipolar cell adaptation.

Remodeling of Second-Order Neurons in Retinal Disease

Under pathologic conditions Cacna1s may also play a role in the remodeling of second-order neurons. Knowledge about the plastic and regenerative capacity of the retina is of key importance for therapeutic approaches to restore vision in patients with degenerative retinal diseases. Although the retinal network transmits in parallel different aspects of vision in a precisely wired fashion, in recent years several reports have described plastic changes of second-order neurons in animal models of photoreceptor degeneration.[62–67] Valuable information was achieved from the detailed descriptions of the spatial and temporal reaction patterns of horizontal and bipolar cells in these animal models. A functional interpretation of the various observed processes in response to a mutation or retinal detachment, however, has been hampered from the relatively rapid disappearance of the photoreceptors. In fact, cell death has been suggested as a trigger for remodeling. Recently, presynaptic synaptopathies as in CSNB2 have come into play as an important factor in sensory system dysfunctions.[12,13,15,16,38] Although degeneration is not the predominant feature, massive outgrowth and remodeling of second-order neurons takes place. Molecular changes associated with the postsynaptic elements that could be involved in triggering outgrowth of second-order neurons under these conditions have not been described so far. The molecular alterations in ON bipolar cell dendritic tips found in this study correlate with remodeling and thus may provide information about candidate molecules and pathways. In particular, Cacna1s may be involved in second-order neuron remodeling via excitation-transcription coupling,[68] regulation of actin dynamics,[69] or mediation of calcium channel–extracellular matrix stop signals.[70]

Effect of Presynaptic Mutations on the Postsynaptic Compartment

We speculate that the postsynaptic changes in the *Bsn*ΔEx4-5 mutant may be exerted via mislocalization of Cacna1f. Although the bona fide horseshoe-shaped distribution of Cacna1f labeling characteristic of mature ribbon synapses never develops in the Bassoon mutant, the Cacna1f protein initially localizes in hot spots. Subsequently, there is a gradual loss of Cacna1f immunoreactivity with age. The initial presence of Cacna1f may suffice to induce and maintain correct localization of mGluR6 and Vlgr1/Gpr98, and to enable residual, short-term Cacna1s labeling. By contrast, expression of these proteins was severely affected in the *Cacna1f*ΔEx14-17 mutant. Thus, the degree of disruption to $Ca_v1.4$ channel function may explain the milder phenotype of the *Bsn*ΔEx4-5 mutant when compared with the *Cacna1f*ΔEx14-17 mutant.

The two previously characterized mouse models with loss-of-function mutations in the *Cacna1f* gene, *Cacna1f*$^{-/-}$, and nob2, also show differences in their phenotypes. Both of these mutants show an absence of normally formed photoreceptor synapses in the OPL, together with formation of ectopic synapses in the ONL. However, in Cacna1f$^{-/-}$ mice signal transmission to higher brain areas was lacking and the ERG b-wave was not detectable, whereas in nob2 mice ganglion cell responses could still be elicited and b-wave amplitude was reduced but measurable.[12,13] A recent study revealed that alternative splicing enables an apparently functional Cacna1f protein to be expressed at low levels in the nob2 mutant.[32] Hence, the key to explaining this phenotypic variability might again lie in the distinct effects of different mutations on Cacna1f protein levels and function.

Consistent with this interpretation, several aspects of the nob2 phenotype resembles that of the Bassoon loss-of-function mutant *Bsn*ΔEx4-5,[15,38] rather than of the *Cacna1f*$^{-/-}$[12] and newly generated *Cacna1f*ΔEx14-17 mutants (this study). mGluR6 localization is retained in the former, and lost in the latter, two mutants.[12,13,71] Similarly, dystrophin, a ligand of the dystroglycan/pikachurin complex involved in ribbon synapse formation[43] is correctly localized in the nob2 mutant,[71] whereas dystroglycan localization was compromised in the *Cacna1f*ΔEx14-17 retina.

We conclude that presynaptic Bassoon and Cacna1f mutations result in severe changes in the molecular composition of both presynaptic and postsynaptic elements of the photoreceptor ribbon synapse. Comparison of the exact molecular changes induced in distinct subsynaptic compartments by different Cacna1f mutations provides a promising tool to unravel steps in photoreceptor synapse formation and maintenance, as well as functional aspects of the mature synapse. Moreover, such studies may explain why the clinical manifestations of different mutations in the human *CACNA1F* gene are highly variable, ranging from relatively mild forms of night blindness to severe forms combined with myopia or hyperopia, nystagmus and diminished visual acuity, symptoms in female carriers, and cone rod dystrophies.[33,72–76]

Acknowledgments

The authors thank Beata Schmidt, Stefanie Heynck, Brigitte Marshall-say, Driss Benzaid, and Gorg-Sun Nam for excellent technical assistance.

References

1. Sterling P, Matthews G. Structure and function of ribbon synapses. *Trends Neurosci.* 2005;28:20–29.
2. tom Dieck S, Brandstätter JH. Ribbon synapses of the retina. *Cell Tissue Res.* 2006;326:339–346.
3. Tachibana M, Okada T, Arimura T, Kobayashi K, Piccolino M. Dihydropyridine-sensitive calcium current mediates neurotransmitter release from bipolar cells of the goldfish retina. *J Neurosci.* 1993;13:2898–2909.
4. Schmitz Y, Witkovsky P. Dependence of photoreceptor glutamate release on a dihydropyridine-sensitive calcium channel. *Neuroscience.* 1997;78:1209–1216.
5. Nachman-Clewner M, Jules RS, Townes-Anderson E. L-type calcium channels in the photoreceptor ribbon synapse: localization and role in plasticity. *J Comp Neurol.* 1999;415:1–16.
6. Brandt A, Khimich D, Moser T. Few Cav1.3 channels regulate the exocytosis of a synaptic vesicle at the hair cell ribbon synapse. *J Neurosci.* 2005;25:11577–11585.
7. Catterall WA, Perez-Reyes E, Snutch TP, Striessnig J. International Union of Pharmacology. XLVIII. Nomenclature and structure-function relationships of voltage-gated calcium channels. *Pharmacol Rev.* 2005;57:411–425.
8. Bech-Hansen NT, Naylor MJ, Maybaum TA, et al. Loss-of-function mutations in a calcium-channel α1-subunit gene in Xp11.23 cause incomplete X-linked congenital stationary night blindness. *Nat Genet.* 1998;19:264–267.
9. Strom TM, Nyakatura G, Apfelstedt-Sylla E, et al. An L-type calcium-channel gene mutated in incomplete X-linked congenital stationary night blindness. *Nat Genet.* 1998;19:260–263.
10. Morgans CW. Localization of the α1F calcium channel subunit in the rat retina. *Invest Ophthalmol Vis Sci.* 2001;42:2414–2418.
11. Morgans CW, Bayley PR, Oesch NW, Ren G, Akileswaran L, Taylor WR. Photoreceptor calcium channels: insight from night blindness. *Vis Neurosci.* 2005;22:561–568.
12. Mansergh F, Orton NC, Vessey JP, et al. Mutation of the calcium channel gene Cacna1f disrupts calcium signaling, synaptic transmission and cellular organization in mouse retina. *Hum Mol Genet.* 2005;14:3035–3046.
13. Chang B, Heckenlively JR, Bayley PR, et al. The nob2 mouse, a null mutation in Cacna1f: anatomical and functional abnormalities in the outer retina and their consequences on ganglion cell visual responses. *Vis Neurosci.* 2006;23:11–24.
14. Ball SL, Powers PA, Shin HS, Morgans CW, Peachey NS, Gregg RG. Role of the β_2 subunit of voltage-dependent calcium channels in the retinal outer plexiform layer. *Invest Ophthalmol Vis Sci.* 2002; 43:1595–1603.
15. Dick O, tom Dieck S, Altrock WD, et al. The presynaptic active zone protein Bassoon is essential for photoreceptor ribbon synapse formation in the retina. *Neuron.* 2003;37:775–786.
16. Haeseleer F, Imanishi Y, Maeda T, et al. Essential role of Ca^{2+}-binding protein 4, a $Ca_v1.4$ channel regulator, in photoreceptor synaptic function. *Nat Neurosci.* 2004;7:1079–1087.
17. Libby RT, Lillo C, Kitamoto J, Williams DS, Steel KP. Myosin Va is required for normal photoreceptor synaptic activity. *J Cell Sci.* 2004;117:4509–4515.
18. Van Epps HA, Hayashi M, Lucast L, et al. The zebrafish nrc mutant reveals a role for the polyphosphoinositide phosphatase synaptojanin 1 in cone photoreceptor ribbon anchoring. *J Neurosci.* 2004; 24:8641–8650.
19. Dryja TP, McGee TL, Berson EL, et al. Night blindness and abnormal cone electroretinogram ON responses in patients with mutations in the GRM6 gene encoding mGluR6. *Proc Natl Acad Sci USA.* 2005;102:4884–4889.
20. Wan L, Almers W, Chen W. Two ribeye genes in teleosts: the role of RIBEYE in ribbon formation and bipolar cell development. *J Neurosci.* 2005;25:941–949.
21. Zeitz C, van Genderen M, Neidhardt J, et al. Mutations in GRM6 cause autosomal recessive congenital stationary night blindness with a distinctive scotopic 15-Hz flicker electroretinogram. *Invest Ophthalmol Vis Sci.* 2005;46:4328–4335.
22. Zeitz C, Kloeckener-Gruissem B, Forster U, et al. Mutations in CABP4, the gene encoding the Ca^{2+}-binding protein 4, cause autosomal recessive night blindness. *Am J Hum Genet.* 2006;79: 657–667.
23. tom Dieck S, Altrock WD, Kessels MM, et al. Molecular dissection of the photoreceptor ribbon synapse: physical interaction of Bassoon and RIBEYE is essential for the assembly of the ribbon complex. *J Cell Biol.* 2005;168:825–836.

24. Koschak A, Reimer D, Walter D, et al. Cav1.4alpha1 subunits can form slowly inactivating dihydropyridine-sensitive L-type Ca^{2+} channels lacking Ca^{2+}-dependent inactivation. *J Neurosci.* 2003; 23:6041–6049.
25. McRory JE, Hamid J, Doering CJ, et al. The CACNA1F gene encodes an L-type calcium channel with unique biophysical properties and tissue distribution. *J Neurosci.* 2004;24:1707–1718.
26. Kamphuis W, Hendriksen H. Expression patterns of voltage-dependent calcium channel α_1 subunit (α_{1A}-α_{1E}) mRNA in rat retina. *Mol Brain Res.* 1998;55:209–220.
27. Morgans CW, Gaughwin P, Maleszka R. Expression of the alpha1F calcium channel subunit by photoreceptors in the rat retina. *Mol Vis.* 2001;7:202–209.
28. Xu HP, Zhao JW, Yang XL. Expression of voltage-dependent calcium channel subunits in the rat retina. *Neurosci Lett.* 2002;329: 297–300.
29. Habermann CJ, O'Brian BJ, Wässle H, Protti D. AII amacrine cells express L-type calcium channels at their output synapses. *J Neurosci.* 2003;23:6904–6913.
30. Krizaj D. Compartmentalization of calcium entry pathways in mouse rods. *Eur J Neurosci.* 2005;22:3292–3296.
31. Xiao H, Chen X, Steele EC Jr. Abundant L-type calcium channel Ca(v) 1.3 (alpha1D) subunit mRNA is detected in rod photoreceptors of the mouse retina via in situ hybridization. *Mol Vis.* 2007; 13:764–771.
32. Doering CJ, Rehak R, Bonfield S, et al. Modified Ca(v)1.4 expression in the Cacna1f(nob2) mouse due to alternative splicing of an ETn inserted in exon 2. *PLoS ONE.* 2008;3:e2538.
33. Hemara-Wahanui A, Berjukow S, Hope CI, et al. A CACNA1F mutation identified in an X-linked retinal disorder shifts the voltage dependence of Cav1.4 channel activation. *Proc Natl Acad Sci USA.* 2005;102:7553–7558.
34. Koentgen F, Suess G, Stewart C, Steinmetz M, Bluethmann H. Targeted disruption of the MHC class IIAa gene in C57BL/6 mice. *Int Immunol.* 1993;5:957–964.
35. Dick O, Hack I, Altrock WD, Garner CC, Gundelfinger ED, Brandstätter JH. Localization of the presynaptic cytomatrix protein Piccolo at ribbon and conventional synapses in the rat retina: comparison with Bassoon. *J Comp Neurol.* 2001;439:224–234.
36. Reiners J, van Wijk E, Märker T, et al. Scaffold protein harmonin (USH1C) provides molecular links between Usher syndrome type 1 and type 2. *Hum Mol Genet.* 2005;14:3933–3943.
37. Altrock WD, tom Dieck S, Sokolov M, et al. Functional inactivation of a fraction of excitatory synapses in mice deficient for the active zone protein Bassoon. *Neuron.* 2003;37:787–800.
38. Specht D, tom Dieck S, Ammermüller J, Regus-Leidig H, Gundelfinger ED, Brandstätter JH. Structural and functional remodeling in the retina of a mouse with a photoreceptor synaptopathy: plasticity in the rod and degeneration in the cone system. *Eur J Neurosci.* 2007;26:2506–2515.
39. Kugler G, Grabner M, Platzer J, Striessnig J, Flucher BE. The monoclonal antibody mAB 1A binds to the excitation-contraction coupling domain in the II-III loop of the skeletal muscle calcium channel alpha(1S) subunit. *Arch Biochem Biophys.* 2004;427:91–100.
40. Grover AK, Khan I. Calcium pump isoforms: diversity, selectivity and plasticity. *Cell Calcium.* 1992;13:9–17.
41. Weston MD, Luijendijk MWJ, Humphrey KD, Möller C, Kimberling WJ. Mutations in the VLGR1 gene implicate G-protein signaling in the pathogenesis of usher syndrome type II. *Am J Hum Genet.* 2004;74:357–366.
42. Ueda H, Gohdo T, Ohno S. β-Dystroglycan localization in the photoreceptor and Müller cells in the rat retina revealed by immunoelectron microscopy. *J Histochem Cytochem.* 1998;46:185–191.
43. Sato S, Omori Y, Katoh K, et al. Pikachurin, a dystroglycan ligand, is essential for photoreceptor ribbon synapse formation. *Nat Neurosci.* 2008;11:923–931.
44. Koulen P, Wei J, Madry C, Liu J, Nixon E. Differentially distributed IP3 receptors and Ca^{2+} signaling in rod bipolar cells. *Invest Ophthalmol Vis Sci.* 2005;46:292–298.
45. Shoshan-Barmatz V, Zakar M, Shmuelivich F, Nahon E, Vardi N. Retina expresses a novel variant of the ryanodine receptor. *Eur J Neurosci.* 2007;26:3113–3125.
46. Sculptoreanu A, Scheuer T, Catterall WA. Voltage-dependent potentiation of L-type Ca^{2+} channels due to phosphorylation by cAMP-dependent protein kinase. *Nature.* 1993;364:240–243.
47. De Waard M, Hering J, Weiss N, Feltz A. How do G proteins directly control neuronal Ca^{2+} channel function? *Trends Pharmacol Sci.* 2005;26:427–436.
48. Balijepalli RC, Foell JD, Hall DD, Hell JW, Kamp TJ. Localization of cardiac L-type Ca(2+) channels to a caveolar macromolecular signaling complex is required for beta(2)-adrenergic regulation. *Proc Natl Acad Sci USA.* 2006;103:7500–7505.
49. Altier C, Zamponi GW. Signaling complexes of voltage-gated calcium channels and G protein-coupled receptors. *J Recept Signal Transduct Res.* 2008;28:71–81.
50. Nakajima Y, Iwakabe H, Akazawa C, et al. Molecular characterization of a novel retinal metabotropic glutamate receptor mGluR6 with a high agonist selectivity for L-2-amino-4-phosphonobutyrate. *J Biol Chem.* 1993;268:11868–11873.
51. Nomura A, Shigemoto R, Nakamura Y, Okamoto N, Mizuno N, Nakanishi S. Developmentally regulated postsynaptic localization of a metabotropic glutamate receptor in rat rod bipolar cells. *Cell.* 1994;77:361–369.
52. Shiells RA, Falk G. Glutamate receptors of rod bipolar cells are linked to a cyclic GMP cascade via a G-protein. *Proc Biol Sci.* 1990;242:91–94.
53. Nawy S, Jahr CE. cGMP-gated conductance in retinal bipolar cells is suppressed by the photoreceptor transmitter. *Neuron.* 1991;7: 677–683.
54. Yamashita M, Wässle H. Responses of rod bipolar cells isolated from the rat retina to the glutamate agonist 2-amino-4-phosphonobutyric acid (APB). *J Neurosci.* 1991;11:2372–2382.
55. Nawy S. The metabotropic receptor mGluR6 may signal through G(o), but not phosphodiesterase, in retinal bipolar cells. *J Neurosci.* 1999;19:2938–2944.
56. Dhingra A, Lyubarsky A, Jiang M, et al. The light response of ON bipolar neurons requires G[alpha]o. *J Neurosci.* 2000;20:9053–9058.
57. Snellman J, Nawy S. Regulation of retinal bipolar cell mGluR6 pathway by calcineurin. *J Neurophysiol.* 2002;88:1088–1096.
58. Snellman J, Nawy S. cGMP-dependent kinase regulates response sensitivity of the mouse on bipolar cell. *J Neurosci.* 2004;24:6621–6628.
59. Shiells RA, Falk G. A rise in intracellular Ca^{2+} underlies light adaptation in dogfish retinal 'on' bipolar cells. *J Physiol.* 1999;514: 343–350.
60. Shiells RA, Falk G. Activation of Ca^{2+}-calmodulin kinase II induces desensitization by background light in dogfish retinal 'on' bipolar cells. *J Physiol.* 2000;528:327–338.
61. Nawy S. Regulation of the on bipolar cell pathway by Ca^{2+}. *J Neurosci.* 2000;20:4471–4479.
62. Peng YW, Hao Y, Petters RM, Wong F. Ectopic synaptogenesis in the mammalian retina caused by rod photoreceptor-specific mutations. *Nat Neurosci.* 2000;11:1121–1127.
63. Strettoi E, Pignatelli V. Modifications of retinal neurons in a mouse model of retinitis pigmentosa. *Proc Natl Acad Sci USA.* 2000;97: 11020–11025.
64. Claes E, Seeliger M, Michalakis S, Biel M, Humphries P, Haverkamp S. Morphological characterization of the retina of the CNGA3(−/−)Rho(−/−) mutant mouse lacking functional cones and rods. *Invest Ophthalmol Vis Sci.* 2004;45:2039–2048.
65. Strettoi E, Mears AJ, Swaroop A. Recruitment of the rod pathway by cones in the absence of rods. *J Neurosci.* 2004;24:7576–7582.
66. Fisher SK, Lewis GP, Linberg KA, Verardo MR. Cellular remodeling in mammalian retina: results from studies of experimental retinal detachment. *Prog Retin Eye Res.* 2005;24:395–431.
67. Beltran WA, Hammond P, Acland GM, Aguirre GD. A frameshift mutation in RPGR exon ORF15 causes photoreceptor degeneration and inner retina remodeling in a model of X-linked retinitis pigmentosa. *Invest Ophthalmol Vis Sci.* 2006;47:1669–1681.
68. Dolmetsch R. Excitation-transcription coupling: signaling by ion channels to the nucleus. *Sci STKE.* 2003;4:1–5.
69. Oertner TG, Matus A. Calcium regulation of actin dynamics in dendritic spines. *Cell Calcium.* 2005;37:477–482.

70. Sann SB, Xu L, Nishimune H, Sanes JR, Spitzer NC. Neurite outgrowth and in vivo sensory innervation mediated by a $Ca_v2.2$-Laminin $\beta2$ stop signal. *J Neurosci.* 2008;28:2366–2374.
71. Bayley PR, Morgans CW. Rod bipolar cells and horizontal cells form displaced synaptic contacts with rods in the outer nuclear layer of the nob2 retina. *J Comp Neurol.* 2007;500:286–298.
72. Boycott KM, Maybaum TA, Naylor MJ, et al. A summary of 20 CACNA1F mutations identified in 36 families with incomplete X-linked congenital stationary night blindness, and characterization of splice variants. *Hum Genet.* 2001;108:91–97.
73. Wutz K, Sauer C, Zrenner E, et al. Thirty distinct CACNA1F mutations in 33 families with incomplete type of XLCSNB and Cacna1f expression profiling in mouse retina. *Eur J Hum Genet.* 2002;10:449–456.
74. Hope CI, Sharp DM, Hemara-Wahanui A, et al. Clinical manifestations of a unique X-linked retinal disorder in a large New Zealand family with a novel mutation in CACNA1F, the gene responsible for CSNB2. *Clin Exp Ophthalmol.* 2005;33:129–136.
75. Jalkanen R, Mäntyjärvi M, Tobias R, et al. X linked cone-rod dystrophy, CORDX3, is caused by a mutation in the CACNA1F gene. *J Med Genet.* 2006;43:699–704.
76. Jalkanen R, Bech-Hansen NT, Tobias R, et al. A novel CACNA1F gene mutation causes Aland Island eye disease. *Invest Ophthalmol Vis Sci.* 2007;48:2498–2502.